

IMPACT OF LAPSE RATES UPON LOW-LEVEL ROTATION IN IDEALIZED STORMS

Matthew D. Parker¹

¹*Department of Marine, Earth, & Atmospheric Sciences, North Carolina State University, Raleigh, NC, USA*

I. INTRODUCTION

A brief survey reveals numerous examples of tornadoes that have occurred in environments with adiabatic, or nearly adiabatic, lapse rates (see, for example, Parker et al 2009, elsewhere in this volume). One reasonable hypothesis for this relationship posits that steeper temperature lapse rates entail more environmental CAPE, which in turn leads to stronger updrafts and enhanced tilting and stretching of vorticity. This process seems relatively straightforward.

However, adiabatic environments are also notable in that they prohibit gravity wave propagation, and in that they provide no resistance to downward parcel displacements. In stable environments, gravity waves quickly disperse convective heating to the far field through propagation. In the absence of such gravity waves, less efficacious dispersion by advection occurs, and a greater fraction of the latent heating remains in the convective column. This can produce comparatively strong subsidence in the immediate near-cloud environment, especially considering the minimal resistance provided by the ambient static stability. This study assessed the response of the flow field to differing environmental lapse rates when the convective heating rate was controlled (held fixed).

II. METHOD

This study used idealized simulations with CM1 (Bryan and Fritsch 2002), v. 12. The model was axisymmetric, dry, frictionless, and excluded Coriolis and radiation effects. The domain was 300 km in the horizontal with an open exterior boundary, and 40 km in the vertical with a wave absorbing layer near the model lid. The grid spacing was a uniform 250 m in both directions. Experiments utilized six different environmental stability profiles (Fig. 1). The model was initialized with a Rankine vortex (based on full physics supercell simulations); it had a 5 km radius of maximum winds. The Rankine vortex was centered at 5.5 km height, with a core vorticity of $.01 \text{ s}^{-1}$. The vertical radius of the vortex was varied among experiments (Fig. 2).

Convection was represented by a constant heat source (based on full physics supercell simulations); it was centered at 5.5 km height and was Gaussian in shape, with a 3 km horizontal radius and a 4.5 km vertical radius. The amplitude at the center of the heat source was 0.1 K s^{-1} . The basic conception of these experiments is much like some past tornado studies (Leslie and Smith 1978, Trapp and Davies-Jones 1997, Markowski et al. 2003, etc.) but the scales here typify a parent storm, not a tornado itself.

III. RESULTS

In the Control vortex simulations, vertical vorticity initially vanishes at the surface (Figs. 2, 3) and air parcels with high angular momentum exist only aloft (Fig. 3). Because there

are no sources of vertical vorticity in the far field, this means that a downdraft is required in order to generate appreciable sub-cloud vorticity. A comparison of the Control vortex experiments (Fig. 4) reveals that such downward advection of the high angular momentum air occurs in the Adiabatic environment (Fig. 1, red) but not in the Base environment (Fig. 1, green). As a result of this increase in surface angular momentum, the large values of vertical vorticity extend to the surface in the Adiabatic experiment (Fig. 4, bottom), but not in the Base experiment (Fig. 4, top).

The physical reason for the differences in Fig. 4 hinges on the near-cloud vertical velocities that are produced in the two environments. After 20 minutes of simulation, the environmental response of the Base experiment is dominated by gravity waves (Fig. 5, top), with the corresponding vertical velocities and temperature anomalies propagating quickly to the far field. In contrast, in the Adiabatic experiment (Fig. 5, bottom), gravity waves are absent from the environment. Instead, the environmental response is in the form of strong subsidence that is anchored very near the outer edge of the convective heat source. This cloud-edge downdraft is responsible for advecting the high angular momentum air downward to the surface, where it then flows inward beneath the convective updraft (Fig. 4).

Time series summaries of all six lapse rate experiments (Fig. 6) show that the three environments with adiabatic lapse rates in the lower troposphere (red, purple, yellow, cf. Fig. 1) produce very similar amounts of surface angular momentum enhancement, whereas the three environments with stabler low-level lapse rates (blue, green, cyan, cf. Fig. 1) produce none. Experiments with an initially elevated vortex (Fig. 2, orange) produce a disparity that is equally striking (Fig. 7).

IV. SUMMARY

When the low-levels are neutrally stratified, heating-induced subsidence is anchored near the cloud edge and is substantially stronger than in a stably stratified layer (Fig. 8). This is partly due to the absence of heating dispersion by gravity waves, and partly due to the weaker resistance to downward parcel displacements. This enhanced heating-induced subsidence can bring high angular momentum air to the surface without the need for evaporative cooling, which may in turn favor tornadogenesis. Additional experiments reveal that when the lateral gradient in heating is sharpened, or the initial vortex is strengthened, the resulting subsidence and surface vorticity are enhanced even further beyond what is shown here.

V. ACKNOWLEDGMENTS

This work was supported by NSF grant ATM-0758509. The author thanks P. Haertel, A. Houston, P. Markowski, J. Nachamkin, and D. Nolan for beneficial discussions.

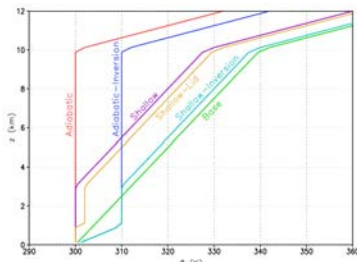


FIG. 1: Profiles of potential temperature used in the experiments.

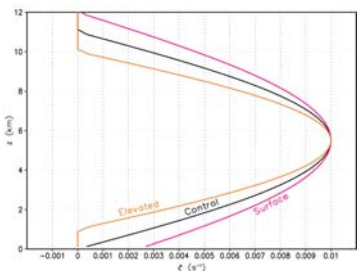


FIG. 2: Profiles of vertical vorticity used in the Rankine vortex.

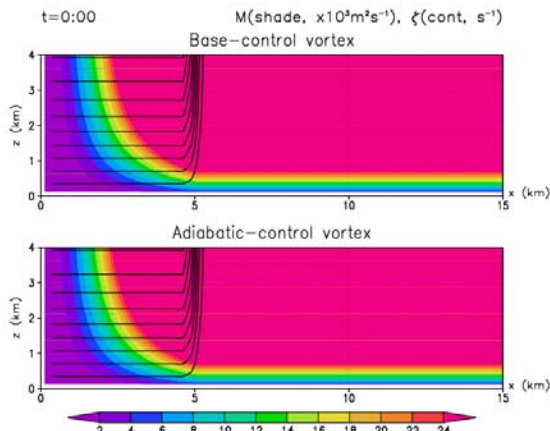


FIG. 3: Initial angular momentum and vertical vorticity for the Control vortex (Fig. 2) experiments.

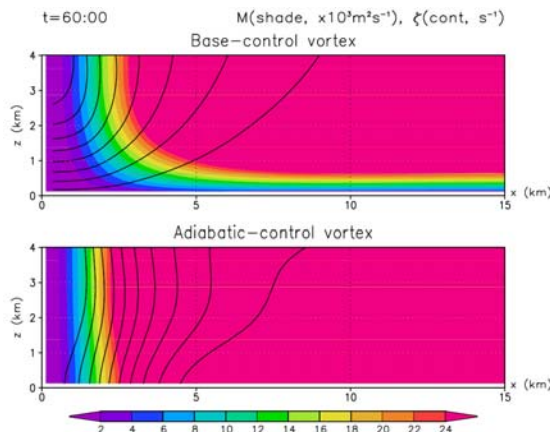


FIG. 4: Same as Fig. 3, except after 1 hour of simulation for the Base (top) and Adiabatic (bottom) lapse rates (Fig. 1).

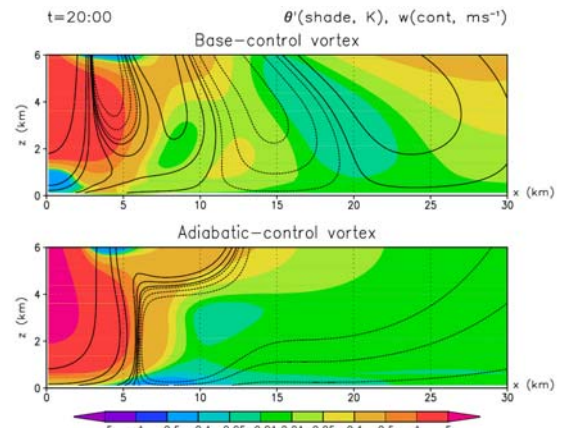


FIG. 5: Same as Fig. 4, except the plotted fields are potential temperature perturbation and vertical velocity after 20 minutes.

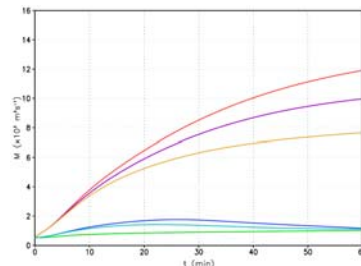


FIG. 6: Time series of mean surface angular momentum within $r=3$ km for the Control vortex experiments (colors correspond to Fig. 1).

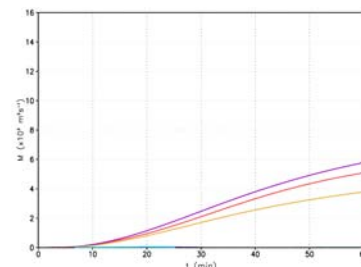


FIG. 7: Same as Fig. 6 except for the Elevated vortex experiments.

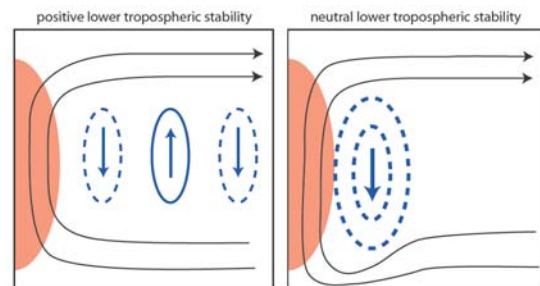


FIG. 8: Conceptual model for the near-storm response in stable vs. adiabatic layers. Heat source is shaded, with transverse circulation in black and near-storm vertical velocities in blue.